MOLECULAR PHYSICS, 1983, VOL. 49, NO. 6, 1385–1400

Anisotropy of the dielectric function within a liquid–vapour interface

by JOHN LEKNER
Physics Department, Victoria University of Wellington, New Zealand

(*Received* 24 *February* 1983 ; *accepted* 2 *April* 1983)

We calculate $\epsilon_\perp(z)$ and $\epsilon_\parallel(z)$, the dielectric functions which characterize the response of a planar interface to an electric field perpendicular to or parallel to the interface. These functions each differ from the Clausius–Mossotti form by an interface term, which depends on the variation in density and in the pair correlation function through the interface. Detailed calculations are carried out for Ar, Kr and Xe, using a molecular dynamics pair correlation function, and three model density profiles. The effect of anisotropy on ellipsometric estimates of the interface thickness is found to be small, because of cancellations between opposing terms.

1. INTRODUCTION

Recent work has shown that even in the simplest case of a lattice [1] or fluid [2] of polarizable atoms, there is some anisotropy of the dielectric function at the solid–vapour and liquid–vapour interfaces. The purpose of this paper is to explore the anisotropy for simple fluids (Ar, Kr and Xe), and the effect of the anisotropy on ellipsometric measurements of the interfacial thickness.

The polarization modulation ellipsometric technique of Jasperson and Schnatterly [3] has been applied by Beaglehole [4] to the determination of interface thickness. The quantity measured is $\tilde{\rho}$, the value of the imaginary part of the ratio of the s and p reflection amplitudes, at the angle where the real part is zero. For light of angular frequency ω, incident from medium 1 onto a planar interface characterized by an isotropic dielectric function $\epsilon(z)$,

$$\tilde{\rho} = \tfrac{1}{2}\frac{\omega}{c}\frac{\sqrt{(\epsilon_1+\epsilon_2)}}{\epsilon_1-\epsilon_2}\eta_0 + \text{terms higher order in interface thickness}, \tag{1}$$

where

$$\eta_0 = \int_{-\infty}^{\infty} dz\,\frac{(\epsilon-\epsilon_1)(\epsilon-\epsilon_2)}{\epsilon} = \int_{-\infty}^{\infty} dz\left\{\epsilon + \frac{\epsilon_1\epsilon_2}{\epsilon} - \epsilon_1 - \epsilon_2\right\}, \tag{2}$$

and ϵ_1 and ϵ_2 are the bulk values of the dielectric function in media 1 and 2. This result, usually credited to Drude [5], was apparently first obtained by L. Lorenz [6] (Rayleigh [7] derives results for a general angle of incidence, and gives reference to the earlier work of Lorenz, Van Ryn, Drude, Schott and Maclaurin). The result of equations (1) and (2) rests on two approximations : neglect of anisotropy and neglect of fluctuations within the interface (surface roughness). The effect of fluctuations has been studied by Zielinska, Bedeaux and Vlieger in a series of papers [8]. The effect of the anisotropy of the dielectric function for a non-fluctuating (or averaged) interface is studied here.

For a planar interface, the reflection of light at a general angle of incidence is determined by two functions, $\epsilon_\perp$ and $\epsilon_\parallel$, representing the response of the system to electric fields applied normally or parallel to the interface, respectively. When anisotropy is taken into account, $\bar{\rho}$ is given by (1), with η_0 replaced by

$$\eta = \int_{-\infty}^{\infty} dz \left\{ \epsilon_\parallel + \frac{\epsilon_1 \epsilon_2}{\epsilon_\perp} - \epsilon_1 - \epsilon_2 \right\}. \tag{3}$$

This formula is derived in Appendix A, using a generalization of a comparison identity derived for isotropic ϵ [9]. A result equivalent to (1) and (3) (apart from its sign) was apparently first given by Buff [10]. Beaglehole [4] extracted the same formula from the work of Abelès [11]. In this paper we shall evaluate (3) using the theory of Castle and Lekner [2] (referred to here as CL).

2. Dielectric functions within the liquid–vapour interface

CL have shown how the local field within a monatomic fluid is related to the external field via the polarizability α of an atom, the number density $n(z)$, and the pair correlation function $g(r, z_1, z_2)$. Within a homogeneous bulk phase, the dielectric function is shown to be (an isotropic) constant, given by the Clausius–Mossotti formula. The assumptions which lead to this result are that (i) the field due to a polarized atom is well approximated by that of a point dipole, and (ii) dipole fluctuations can be neglected. These assumptions are discussed further in [1] and [2]; they are justified to some extent by the very small variation in the effective atomic or molecular polarizabilities found from the Lorenz–Lorentz or Clausius–Mossotti formulae in a variety of gases, liquids and solids under a wide range of conditions [12].

Within the interfacial region, CL show that the dielectric functions are well approximated by the Clausius–Mossotti form

$$\epsilon_{\mathrm{CM}}(z_1) = \frac{1 + \frac{8}{3}\pi\alpha n(z_1)}{1 - \frac{4}{3}\pi\alpha n(z_1)}, \tag{4}$$

with a small correction arising from inhomogeneity. From CL (14), (20), and (23) we find

$$\epsilon_\perp(z_1) = \frac{1 + \frac{8}{3}\pi\alpha n(z_1) + I(z_1)}{1 - \frac{4}{3}\pi\alpha n(z_1) + I(z_1)}, \tag{5}$$

where the interfacial contribution I is given by

$$I(z_1) = -2\pi\alpha \int_0^\infty dr\, r^{-4} \int_{-r}^{r} dz (3z^2 - r^2) n(z_1 + z)[g(r, z_1, z_1 + z) - 1] \tag{6}$$

(the interface lies in the x–y plane; z_1 and z_2 are depth coordinates of atoms 1 and 2, $r = |\mathbf{r}_2 - \mathbf{r}_1|$ is the distance between the two atoms, and $z = z_2 - z_1$ is the difference in their depths).

A result similar to (5) is obtained in the case where the electric field is parallel to the interface. From CL (40) and the general definition of ϵ (see CL, Note Added in Proof), we find

$$\epsilon_\parallel(z_1) = \frac{1 + \frac{8}{3}\pi\alpha n(z_1) - \frac{1}{2} I(z_1)}{1 - \frac{4}{3}\pi\alpha n(z_1) - \frac{1}{2} I(z_1)}. \tag{7}$$

Thus the correction to the Clausius–Mossotti form is opposite sign (at any particular z_1) for $\epsilon_\perp$ and $\epsilon_\parallel$, and is twice as large for $\epsilon_\perp$.

To evaluate I we need the number density $n(z)$, and the generalized pair correlation function $g(r, z_1, z_2)$ within the interfacial region. Without loss of generality we can write g as a linear combination of $g_l(r)$ and $g_v(r)$ (the pair correlation functions within the liquid and vapour phases), weighted by the density at the mean depth $\bar{z}=\frac{1}{2}(z_1+z_2)$, plus a correction term Δg :

$$g(r, z_1, z_2)=\frac{n(\bar{z})-n_v}{n_l-n_v}\,g_l(r)+\frac{n_l-n(\bar{z})}{n_l-n_v}\,g_v(r)+\Delta g(r, z_1, z_2). \tag{8}$$

Since g, g_l and g_v all tend to zero as $r\to 0$ and to unity as $r\to\infty$, Δg is zero at both small r and large r. Lekner and Henderson [13] used this form for g, with $\Delta g=0$ and with $\Delta g=[g_l(r)-g_v(r)]F(\bar{z})$, to obtain the pressure/temperature ratio along the coexistence curve as a function of n_l and n_v. The comparison of their results with experimental data is consistent with Δg being small, and in the remainder of this paper we shall set it equal to zero.

The density profile $n(z)$ is conveniently written in the form

$$n(z)=\tfrac{1}{2}(n_l+n_v)-\tfrac{1}{2}(n_l-n_v)\theta(z), \tag{9}$$

where $\theta(\pm\infty)=\pm 1$. In terms of θ, and with $\Delta g=0$,

$$g(r, z_1, z_2)\simeq\tfrac{1}{2}[g_l(r)+g_v(r)]-\tfrac{1}{2}[g_l(r)-g_v(r)]\theta(\bar{z}). \tag{10}$$

Using (9) and (10) in (6) we find

$$\begin{aligned} I(z_1)\simeq\pi\alpha\int_0^\infty dr\,r^{-4}\int_{-r}^{r}dz\,(3z^2-r^2)\Big\{&(n_l-n_v)[\bar{g}(r)-1]\theta(z_1+z)\\ &+\bar{n}[g_l(r)-g_v(r)]\theta\left(z_1+\frac{z}{2}\right)-\tfrac{1}{2}(n_l-n_v)\\ &\times[g_l(r)-g_v(r)]\theta(z_1+z)\theta\left(z_1+\frac{z}{2}\right)\Big\}, \end{aligned} \tag{11}$$

where

$$\bar{n}=\tfrac{1}{2}(n_l+n_v),\quad \bar{g}(r)=\tfrac{1}{2}[g_l(r)+g_v(r)]. \tag{12}$$

We shall write (12) as $I=I_n+I_g+I_{ng}$, where the subscripts n, g, and ng denote contributions to the inhomogeneity term from variation through the interface of density, pair correlations, and density and pair correlations together. We have

$$\left.\begin{aligned} I_n(z_1)&=\pi\alpha(n_l-n_v)\int_0^\infty dr\,r^{-4}[\bar{g}(r)-1]K_n(r, z_1),\\ I_g(z_1)&=\pi\alpha\bar{n}\int_0^\infty dr\,r^{-4}[g_l(r)-g_v(r)]K_g(r, z_1),\\ I_{ng}(z_1)&=-\frac{\pi}{2}\,\alpha(n_l-n_v)\int_0^\infty dr\,r^{-4}[g_l(r)-g_v(r)]K_{ng}(r, z_1), \end{aligned}\right\} \tag{13}$$

where

$$\left.\begin{aligned} K_n(r, z_1)&=\int_{-r}^{r}dz\,(3z^2-r^2)\theta(z_1+z),\\ K_g(r, z_1)&=\int_{-r}^{r}dz\,(3z^2-r^2)\theta\left(z_1+\frac{z}{2}\right),\\ K_{ng}(r, z_1)&=\int_{-r}^{r}dz\,(3z^2-r^2)\theta(z_1+z)\theta\left(z_1+\frac{z}{2}\right). \end{aligned}\right\} \tag{14}$$

When θ is odd (as it is for the model density profiles considered here), K_n and K_g are odd functions of z_1, and K_{ng} is an even function of z_1. If the first three integrals of θ are known, K_n and K_g may be evaluated by repeated integration by parts : let

$$\theta=\frac{d}{dz}\,\theta_1=\frac{d^2}{dz^2}\,\theta_2=\frac{d^3}{dz^3}\,\theta_3. \tag{15}$$

Then

$$K_n(r,z_1)=2r^2[\theta_1(z_1+r)-\theta_1(z_1-r)]-6r[\theta_2(z_1+r)+\theta_2(z_1-r)] +6[\theta_3(z_1+r)-\theta_3(z_1-r)] \tag{16}$$

and

$$K_g(r,z_1)=4r^2\left[\theta_1\left(z_1+\frac{r}{2}\right)-\theta_1\left(z_1-\frac{r}{2}\right)\right]-24r\left[\theta_2\left(z_1+\frac{r}{2}\right) +\theta_2\left(z_1-\frac{r}{2}\right)\right]+48\left[\theta_3\left(z_1+\frac{r}{2}\right)-\theta_3\left(z_1-\frac{r}{2}\right)\right]. \tag{17}$$

CL estimated I_n for the exponential profile (to be discussed in § 5), approximating $\bar{g}(r)$ by $g_v(r)$; and neglected I_g and I_{ng}. We shall explore the relative importance of I_n, I_g and I_{ng} in the next three sections, using in sequence three model density profiles. For the pair correlation functions we shall use $g_v(r)=\exp(-u(r)/T)$, where the interatomic potential $u(r)$ is taken to be of the Lennard-Jones 6-12 form

$$u(r)=4v\left[\left(\frac{d}{r}\right)^{12}-\left(\frac{d}{r}\right)^{6}\right], \tag{18}$$

and the numerical $g_l(r)$ of Verlet [14] (table 4). This was produced by a molecular dynamics simulation on a model 6-12 fluid ; the $g_l(r)$ used here is for $n_l d^3=0{\cdot}850$, $T/v=0{\cdot}719$, which is the closest to the triple point ($n_l d^3\simeq 0{\cdot}84$, $T/v\simeq 0{\cdot}70$) among the Verlet data. The potential strengths v, atomic diameters d (for the 6-12 fluid), and atomic polarizabilities α of argon, krypton and xenon are given in table 1. We also give the experimental liquid and vapour densities at the temperature $T=0{\cdot}719\,v$ for which the liquid pair correlation function is tabulated. Since the dielectric properties depend strongly on the product of the atomic polarizability and density, we have used the experimental liquid densities in preference to $0{\cdot}85/d^3$ in our calculations.

Table 1. Data used in the calculation of dielectric functions

	Ar	Kr	Xe	Reference
v(K)	117·2	163·1	226·1	[15]
0·719 v(K)	84·3	117·3	162·6	
d(Å)	3·405	3·634	3·954	[15]
$0{\cdot}85/d^3$(Å^{-3})	0·02153	0·01771	0·01375	
n_l(Å^{-3})	0·02128	0·01747	0·01356	[16–18]
n_v(Å^{-3})	0·00006	0·00005	0·00004	[16–18]
α(Å^3)	1·62	2·46	3·99	[19]

The pair correlation functions $g_l(r)$ and $g_v(r)$ are shown in figure 1. The difference $g_l(r)-g_v(r)$ (figure 2) is seen to have a substantial negative region, which suggests that I_g and I_{ng} may not be negligible.

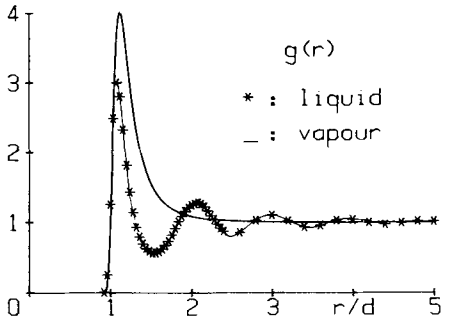

Figure 1. Pair correlation functions in the liquid and vapour phases.

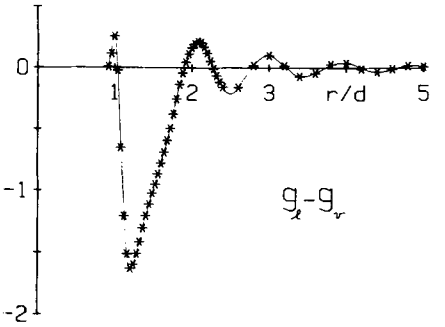

Figure 2. The difference between the liquid and vapour pair correlation functions.

3. η FOR THE STEP PROFILE

The step profile, for which $n(z)=n_l$ $(z<0)$ and $n(z)=n_v$ $(z>0)$, and

$$\theta(z)=\text{sgn}\,(z), \tag{19}$$

is a physically inconsistent model density to use with the pair correlation functions shown above. It is interesting however as a limiting case, in which the entire contribution to the ellipsometric quantity η is due to anisotropy (η_0 is zero for the step profile). From (16) and

$$\theta_1(z)=|z|, \quad \theta_2(z)=\tfrac{1}{2}z^2\,\text{sgn}\,(z), \quad \theta_3(z)=\tfrac{1}{6}|z|^3, \tag{20}$$

or by direct integration, we find

$$K_n(r, z_1)=\begin{cases} 2z_1(z_1^2-r^2), & r>|z_1|, \\ 0 \quad , & r<|z_1| \end{cases} \tag{21}$$

and

$$K_g(r, z_1)=\begin{cases} 4z_1(4z_1^2-r^2), & r>2|z_1|, \\ 0 \quad , & r<2|z_1|. \end{cases} \tag{22}$$

By an integration by parts, K_{ng} is transformed into

$$K_{ng}(r, z_1) = 2\int_{-r}^{r} dz\, z(r^2 - z^2)\{\delta(z_1 + z)\,\mathrm{sgn}\,(2z + z) + \delta(2z_1 + z)\,\mathrm{sgn}\,(z_1 + z)\}$$

$$= [K_n(r, z_1) - K_g(r, z_1)]\,\mathrm{sgn}\,(z_1). \tag{23}$$

The discontinuity in density leads to a discontinuity in $I_n(z_1)$ at $z_1 = 0$:

$$I_n(z_1) \to \tfrac{4}{3}\pi\alpha(n_1 - n_v)\,\mathrm{sgn}\,(z_1) \quad \text{as} \quad z_1 \to 0. \tag{24}$$

I_g and I_{ng} are continuous (and both zero) at $z_1 = 0$, because the factor $g_l(r) - g_v(r)$ removes the singular contribution from small r values. The xenon values for I_n and I_g (odd) and I_{ng} (even) are shown for positive z in figure 3 and the total interface term I is shown in figure 4; they are an order of magnitude larger for this discontinuous profile than for the continuous profiles to be discussed. The values of η (table 2) are nevertheless comparable to those for the more realistic profiles, because of the absence of an isotropic contribution. For xenon the contributions of I_n alone, I_g alone and I_{ng} alone amount to respectively 51, 32 and 32 per cent of the total (these do not add to 100 per cent because η is not linear in I). The effect of I_g and I_{ng} is thus substantial in this example.

Table 2. Values of η and η_0 (obtained by setting $I \equiv 0$), near the triple point of Ar, Kr and Xe. (Three or four digits are given, for the comparison of *relative* magnitudes. For *absolute* magnitudes, at best the leading non-zero digit is sufficient—see for example the range of estimates of interface thickness shown in table 1 of [23]).

Profile		Ar	Kr	Xe
step	$-\eta/d$	0·0276	0·0443	0·0735
linear	$-\eta/d$	0·0625	0·1003	0·1667
$a_l = 0{\cdot}9d$	$-\eta_0/d$	0·0617	0·0991	0·1647
	η/η_0	1·013	1·012	1·012
exponential	$-\eta/d$	0·0672	0·1080	0·1797
$a_e = 0{\cdot}425d$	$-\eta_0/d$	0·0657	0·1056	0·1759
	η/η_0	1·023	1·023	1·022

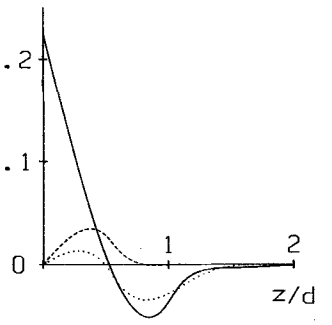

Figure 3. Interfacial terms I_n(———), I_g(- - - - -) and I_{ng}(· · · · · ·) for the step profile.

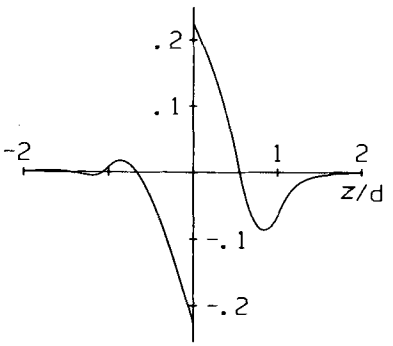

Figure 4. Total interfacial contribution for the step density profile.

4. η FOR THE LINEAR PROFILE

The linear density profile, for which $\theta(z)=z/a$ ($|z|<a$), $\theta(z)=\mathrm{sgn}\,(z)$ ($|z|>a$), is the simplest continuous model for density variation across the interface. Shih and Uang [20] have used this profile, among others, to calculate the surface tension σ and the surface energy ϵ for argon at 85 K. Henderson and Lekner [21] have used these calculations to extract an interface thickness; in terms of the parameter a defined above, they find $a\simeq 0{\cdot}9\,d$. We shall use this value in our calculations. We need K_n, K_g and K_{ng}. For the linear profile we have

$$\left.\begin{aligned} \theta_1(z)&=\tfrac{1}{2}z^2/a+\tfrac{1}{2}a\,; && |z|,\\ \theta_2(z)&=\tfrac{1}{6}z^3/a+\tfrac{1}{2}az\,; && (\tfrac{1}{2}z^2+\tfrac{1}{6}a^2)\ \mathrm{sgn}\ (z),\\ \theta_3(z)&=\tfrac{1}{24}z^4/a+\tfrac{1}{4}az^2+\tfrac{1}{24}a^3\,; && \tfrac{1}{6}|z|^3+\tfrac{1}{6}a^2|z|, \end{aligned}\right\} \tag{25}$$

where the forms on the left are for $|z|<a$, those on the right for $|z|>a$. From (16) and (25), or by direct integration, we find

$$K_n(r,z_1)=\begin{cases}\dfrac{1}{4a}\,(u_n^2-l_n^2)(2r^2-u_n^2-l_n^2), & \text{if}\quad l_n<u_n,\\ 0, & \text{if}\quad l_n>u_n,\end{cases} \tag{26}$$

where

$$l_n=-\min\,(r,\,a+z_1),\quad u_n=\min\,(r,\,a-z_1). \tag{27}$$

Similarly,

$$K_g(r,z_1)=\begin{cases}\dfrac{1}{8a}\,(u_g^2-l_g^2)(2r^2-u_g^2-l_g^2), & \text{if}\quad l_g<u_g,\\ 0, & \text{if}\quad l_g>u_g,\end{cases} \tag{28}$$

where

$$l_g=-\min\,(r,\,2a+2z_1),\quad u_g=\min\,(r,\,2a-2z_1). \tag{29}$$

$K_{ng}(r,z_1)$ may be evaluated by integration by parts. The result is

$$K_{ng}(r,z_1)=A(r,z_1,z)\big|_{l_n}^{u_n}+B(r,z_1,z)\big|_{l_g}^{u_g}+C(r,z)\big|_{l}^{u}\,, \tag{30}$$

where

$$\left.\begin{aligned} A(r, z_1, z) &= \frac{z^2}{4a}(2r^2 - z^2)\theta(z_1 + z/2), \\ B(r, z_1, z) &= \frac{z^2}{8a}(2r^2 - z^2)\theta(z_1 + z), \\ C(r, z) &= -\frac{z^3}{4a^2}(\tfrac{2}{3}r^2 - \tfrac{1}{5}z^2), \\ l = \max(l_n, l_g), &\quad u = \min(u_n, u_g) \end{aligned}\right\} \tag{31}$$

and where each term of (30) is to be given zero value when the lower limit exceeds the upper limit.

For analytic density profiles, the r^{-4} term in $I_n(z_1)$ does not lead to a singularity at small r : expansion of $\theta(z_1+z)$ about z_1 shows that

$$I_n(z_1) = \tfrac{4}{15}\pi\alpha(n_1 - n_v)\theta''(z_1)\int_0^\infty dr\, r(\bar{g}(r) - 1) + \dots . \tag{32}$$

We have already seen in the case of the step profile that a discontinuity in density, together with the short-ranged r^{-4} behaviour of the r-integrand, leads to a discontinuity in $I_n(z_1)$ at $z_1 = 0$ (the point of discontinuity in density). The linear profile has a discontinuity in slope at $z_1 = \pm a$, and this leads to a discontinuity in the slope of $I_n(z_1)$ at $z_1 = \pm a$. From (16), we have

$$\begin{aligned} \frac{dI_n(z_1)}{dz_1} = \pi\alpha(n_1 - n_v)\int_0^\infty dr r^{-4}(\bar{g}(r) - 1)\{2r^2[\theta(z_1 + r) - \theta(z_1 - r)] \\ - 6r[\theta_1(z_1 + r) + \theta_1(z_1 - r)] + 6[\theta_2(z_1 + r) - \theta_2(z_1 - r)]\}. \end{aligned} \tag{33}$$

For $z_1 = a + \delta$ and $|\delta| < r < 2a + \delta$ the expression in braces becomes $\delta r^2/a + O(\delta^2)$. When $r < |\delta|$ and $r < 2a + \delta$ it takes the value zero. The consequent value of dI_n/dz_1 at $z_1 = a + \delta$ is $-\pi\alpha(n_1 - n_v)\,\mathrm{sgn}(\delta)/a$, giving a discontinuity in the slope of I_n of $2\pi\alpha(n_1 - n_v)/a$. The behaviour near $z_1 = -a$ follows from the above and the fact that $I_n(z_1)$ is odd when $\theta(z)$ is odd.

The xenon values for I_n, I_g and I_{ng} are shown in figure 5, and the total I in figure 6 ; the discontinuity in slope at $|z_1| = a$ is apparent. The values of η obtained with this profile for Ar, Kr, Xe are given in table 2. I_n, I_g and I_{ng} separately give a -6, $+4$ and $+3$ per cent correction to η_0 ; the total I gives a $+1$ per cent correction.

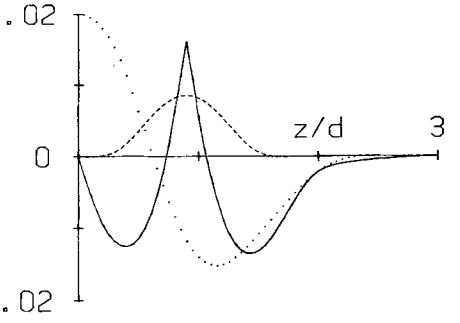

Figure 5. Interfacial terms I_n(———), I_g(- - - - -) and I_{ng}(· · · · · ·) for the linear profile.

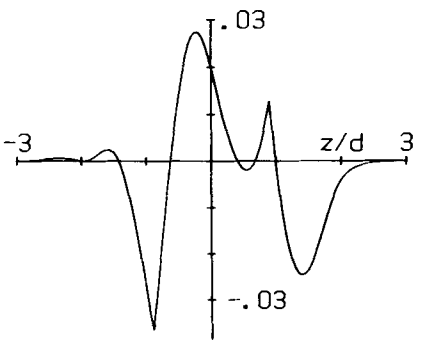

Figure 6. Total interfacial contribution for the linear density profile.

5. η FOR THE EXPONENTIAL PROFILE

The exponential profile is the most realistic of the model profiles considered here, and yet has the advantage that much of the required integration can be done analytically, both in the statistical mechanical expressions for the surface tension and surface energy [22], and also in the statistical mechanics of dielectric properties [2]. For this profile,

$$\left.\begin{aligned}\theta(z) &= [1-\exp(-|z|/a)]\,\mathrm{sgn}\,(z),\\ \theta_1(z) &= |z| + a\exp(-|z|/a),\\ \theta_2(z) &= [\tfrac{1}{2}z^2 + a^2(1-\exp(-|z|/a)]\,\mathrm{sgn}\,(z),\\ \theta_3(z) &= \tfrac{1}{6}|z|^3 + a^2|z| + a^3\exp(-|z|/a).\end{aligned}\right\} \tag{34}$$

The length a appropriate to $T/v = 0{\cdot}0703$ was determined in [23] to be approximately $0{\cdot}415\ d$ (this number was obtained as a mean over two methods, and by averaging over Ar, Kr and Xe data). The corresponding 10–90 thickness [23] is $t = (2\log 5)a \simeq 1{\cdot}34\ d$. Later calculations based on more realistic pair correlation functions confirmed that t is approximately 1·3 atomic diameters for argon near its triple point [21]. The densities and pair correlations used here

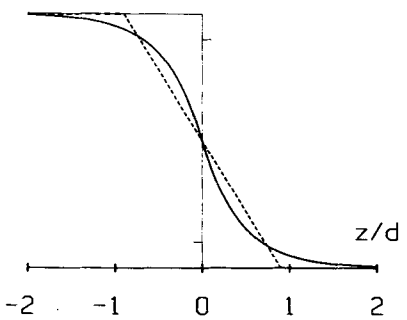

Figure 7. The exponential (———), linear (- - - - -) and step (thin line) density profile used in the calculation of η (table 2). Also shown are markers at $\frac{9}{10}n_l + \frac{1}{10}n_v$ and $\frac{1}{10}n_l + \frac{9}{10}n_v$ to indicate the determination of the 10–90 thickness t.

are for $T/v = 0{\cdot}719$. We have correspondingly used a slightly larger value $a = 0{\cdot}425\ d$, obtained from the scaling law [24]

$$a(T) = a(T_t)\left(\frac{T_c - T_t}{T_c - T}\right)^{\nu}, \tag{35}$$

with $\nu = 2/3$, $T_c/v = 1{\cdot}24$, $T_t/v = 0{\cdot}70$. The resultant 10–90 thickness is $t \simeq 1{\cdot}37\ d$. The linear profile value corresponding to $a_1 = 0{\cdot}9\ d$ is slightly larger ($t \simeq 1{\cdot}44\ d$); the two profiles are compared in figure 7.

The functions K_n and K_g may be obtained from (16), (17) and (34). K_{ng} was evaluated by numerical integration. The xenon values for I_n, I_g and I_{ng} are shown in figure 8, and the total I in figure 9. The values of η obtained with this profile for Ar, Kr and Xe are given in table 2. I_n, I_g and I_{ng} separately give a -5, $+4$ and $+4$ per cent correction to η_0; the total I gives a $+2$ per cent correction. These contributions are similar to those for the linear profile, despite the cusp in $I_n(z_1)$ due to the discontinuity in slope in the linear case.

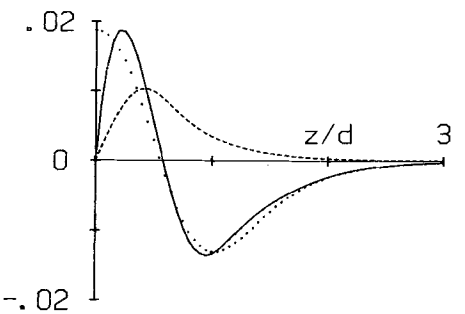

Figure 8. Interfacial terms I_n(———), I_g(- - - -) and I_{ng}(· · · · ·) for the exponential profile.

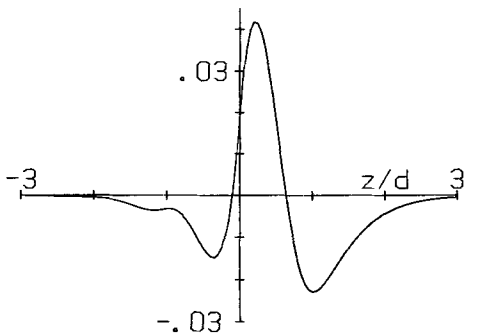

Figure 9. Total interfacial contribution for the exponential density profile.

6. Temperature dependence

Among the Verlet $g_1(r)$ data there is one other set of pair correlation function values lying near the liquid–vapour coexistence curve. This is at $nd^3 = 0{\cdot}65$, $T/v = 1{\cdot}036$. The length a_e at this temperature takes the value $0{\cdot}794\ d$ according to (35), i.e. nearly twice the value assigned to it near the triple point. The

densities used in the calculation of η values are shown in table 3. As in the previous calculations, we have used the experimental densities for the liquid in preference to the value $0{\cdot}65/d^3$ used in the molecular dynamics simulation. The results (table 3) show a small increase in the value of η, and a decrease in the effect of anisotropy. The small change in the value of η despite the near doubling of the interface thickness t can be understood from the approximate proportionality (Appendix B) of η_0 to $(\epsilon_l-\epsilon_v)^2\,t$. As we move from the triple point toward the critical point, $\epsilon_l-\epsilon_v$ and t obey (asymptotically) the scaling laws [24] $\epsilon_l-\epsilon_v\sim(T_c-T)^\beta$, $t\sim(T_c-T)^{-\nu}$. Since $2\beta\simeq\nu$, the respective contributions to η_0 approximately cancel. This is shown in figure 10: the η integrand has longer range but smaller maximum value at the higher temperature.

Table 3. Values of η for the exponential profile at $T=1{\cdot}036\,v$, with $a_e=0{\cdot}794\,d$. The density data are from the references of table 1.

	Ar	Kr	Xe
$1{\cdot}036\,v$(K)	121·4	169·0	234·2
$0{\cdot}65/d^3$(Å^{-3})	0·01647	0·01354	0·01051
n_l(Å^{-3})	0·01730	0·01415	0·01098
n_v(Å^{-3})	0·00098	0·00087	0·00063
$-\eta/d$	0·0722	0·1132	0·1876
$-\eta_0/d$	0·0711	0·1115	0·1849
η/η_0	1·015	1·015	1·015

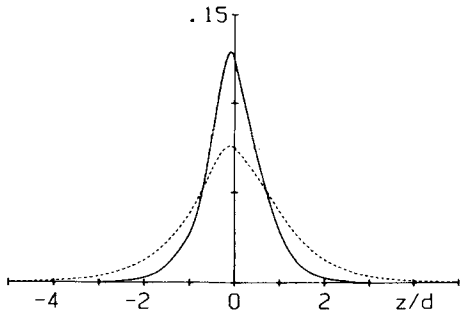

Figure 10. Integrand of $-\eta$ at $T=0{\cdot}719v$ (———) and $T=1{\cdot}036v$ (- - - -).

7. Discussion

The numerical values for $\epsilon_\perp$ and $\epsilon_\parallel$ of CL, based on approximating the pair correlation function by its dilute gas limit, lead to $\eta/\eta_0\simeq 0{\cdot}8$ near the triple point of Ar, Kr and Xe. This apparent 20 per cent decrease in the magnitude of η has been shown here to be not only an overestimate, but even of the wrong sign. The more realistic estimates of the pair correlation function give three contributions to the interface or inhomogeneity term I; of these I_n was overestimated by CL, and the two other terms I_g and I_{ng} (neglected by CL) both contribute to η in opposition to I_n. The net result is a small increase of 2

per cent in the magnitude of η. These results appear surprising at first, since the density changes by a factor of about 350 on passing from vapour to liquid (for Ar near the triple point), while the pair correlation function suffers a moderate change (figure 1). The explanation lies in the fact that a structureless fluid ($g \equiv 1$) would have an isotropic dielectric function, of the Clausius–Mossotti form, no matter how large the change of density at the interface (see (5–7)). The deviation of g from unity is thus all-important, and moderate changes in g through the interface lead to appreciable effects. Because of a large amount of cancellation, the overall change in η due to anisotropy is seen to be negligible for monatomic fluids. This makes it a plausible first approximation to neglect such non-orientational anisotropy in estimates of η due to molecular orientation at the interface [25].

Appendix A

Reflection of light by a planar liquid–vapour interface

For the s-wave, in which the electric field is perpendicular to the plane of incidence (here the zx plane), $\mathbf{E} = (0, E_y, 0)$ and E_y satisfies

$$\nabla^2 E_y + \epsilon_{\parallel} \frac{\omega^2}{c^2} E_y = 0. \tag{A 1}$$

The operative dielectric function for the s-wave is $\epsilon_{\parallel}$, since the electric field is always parallel to the surface. When $\epsilon_{\parallel}$ is purely a function of z (which is the assumption here), $E_y = \exp(iKx)E(z)$, where $E(z)$ satisfies

$$\frac{d^2 E}{dz^2} + \left(\epsilon_{\parallel} \frac{\omega^2}{c^2} - K^2 \right) E = 0 \tag{A 2}$$

and $K = \sqrt{\epsilon_1}(\omega/c) \sin\theta_1 = \sqrt{\epsilon_2}(\omega/c) \sin\theta_2$. The s-wave reflection amplitude is then given by [26]

$$r_s = \frac{q_1 - q_2}{q_1 + q_2} \left\{ 1 - 4q_1 q_2 \int_{-\infty}^{\infty} dz\, z \frac{\epsilon_{\parallel} - \epsilon_0}{\epsilon_1 - \epsilon_2} \right\} + O(qa)^3 \tag{A 3}$$

where $q_i = \sqrt{\epsilon_i}(\omega/c) \cos\theta_i$ and the step dielectric function $\epsilon_0 = \frac{1}{2}(\epsilon_1 + \epsilon_2) - \frac{1}{2}(\epsilon_1 - \epsilon_2)\,\mathrm{sgn}\,(z)$ is located so as to make

$$\int_{-\infty}^{\infty} dz\, (\epsilon_{\parallel} - \epsilon_0) = 0. \tag{A 4}$$

Thus r_s is given by the step value $r_0 = (q_1 - q_2)/(q_1 + q_2)$ to the zeroth and first orders in the interface thickness (characterized by the length a), when the step reference profile is at $z = 0$ and (A 4) is satisfied.

For the p-wave, $\mathbf{B} = (0, B_y, 0)$ and

$$\frac{\partial B_y}{\partial z} = i\epsilon_{\parallel} \frac{\omega}{c} E_x, \quad \frac{\partial B_y}{\partial x} = -i\epsilon_{\perp} \frac{\omega}{c} E_z. \tag{A 5}$$

These equations are the anisotropic generalizations of the usual time-harmonic relation $\nabla \times \mathbf{B} = -i\epsilon(\omega/c)\mathbf{E}$. From the complementary relation $\nabla \times \mathbf{E} = i(\omega/c)\mathbf{B}$ we find

$$\frac{\partial E_x}{\partial z} - \frac{\partial E_z}{\partial x} = i \frac{\omega}{c} B_y. \tag{A 6}$$

All fields have exp (iKx) as the x-dependence, so (A 5) and (A 6) reduce to

$$\frac{d}{dz}\left(\frac{1}{\epsilon_{\parallel}}\frac{dB}{dz}\right)+\left(\frac{\omega^2}{c^2}-\frac{K^2}{\epsilon_{\perp}}\right)B=0, \tag{A 7}$$

where $B_y(z, x)=\exp(iKx)B(z)$. The corresponding equation for an isotropic $\epsilon(z)$ is [27]

$$\frac{d}{dz}\left(\frac{1}{\epsilon}\frac{dB}{dz}\right)+\left(\frac{\omega^2}{c^2}-\frac{K^2}{\epsilon}\right)B=0. \tag{A 8}$$

To find the reflection amplitude r_p to first order in the interface thickness, we will use a generalization of the comparison identity derived in [9]. This identity is derived by multiplying (A 7) by B_0, the solution of (A 8) with $\epsilon=\epsilon_0$, and subtracting from this the complementary expression. We find

$$\frac{d}{dz}(B_0C-BC_0)=K^2\left(\frac{1}{\epsilon_{\perp}}-\frac{1}{\epsilon_0}\right)BB_0-(\epsilon_{\parallel}-\epsilon_0)CC_0, \tag{A 9}$$

where

$$C=\frac{1}{\epsilon_{\parallel}}\frac{dB}{dz} \quad \text{and} \quad C_0=\frac{1}{\epsilon_0}\frac{dB_0}{dz}. \tag{A 10}$$

On integrating (A 9) from $z=-\infty$ to ∞ and using the asymptotic form [9]

$$\exp(iq_1z)-r_p\exp(-iq_1z)\leftarrow B(z)\rightarrow\sqrt{\frac{\epsilon_2}{\epsilon_1}}\,t_p\exp(iq_2z), \tag{A 11}$$

we find the comparison identity for an anisotropic system :

$$r_p=r_{p0}+\frac{1}{2iQ_1}\int_{-\infty}^{\infty}dz\left\{\left(\frac{1}{\epsilon_0}-\frac{1}{\epsilon_{\perp}}\right)K^2BB_0+(\epsilon_{\parallel}-\epsilon_0)CC_0\right\}. \tag{A 12}$$

Here $Q_i=q_i/\epsilon_i$. To lowest order in the interface thickness, we can replace BB_0 by $B_0^2(0)$ and CC_0 by $C_0^2(0)$ in the integrand. The second term in the integral is zero because of (A 4), so with $B_0(0)=2Q_1/(Q_1+Q_2)$ ((58) of [9]) we find

$$r_p=\frac{Q_2-Q_1}{Q_2+Q_1}-\frac{2_iQ_1K^2\,D}{(Q_1+Q_2)^2}+O(qa)^2, \tag{A 13}$$

where the length D is given by

$$D=\int_{-\infty}^{\infty}dz\left(\frac{1}{\epsilon_0}-\frac{1}{\epsilon_{\perp}}\right). \tag{A 14}$$

Using (A 4), D may be written in three equivalent forms, all of which explicitly display the necessary invariance of r_p/r_s with respect to the choice of origin :

$$\begin{aligned}\epsilon_1\epsilon_2D&=\int_{-\infty}^{\infty}dz\left\{\epsilon_1+\epsilon_2-\frac{\epsilon_1\epsilon_2}{\epsilon_{\perp}}-\epsilon_{\parallel}\right\}\\&=\int_{-\infty}^{\infty}dz\,\frac{(\epsilon_1-\epsilon_{\perp})(\epsilon_{\perp}-\epsilon_2)}{\epsilon_{\perp}}+\int_{-\infty}^{\infty}dz\,(\epsilon_{\perp}-\epsilon_{\parallel})\\&=\int_{-\infty}^{\infty}dz\,\frac{(\epsilon_1-\epsilon_{\parallel})(\epsilon_{\parallel}-\epsilon_2)}{\epsilon_{\parallel}}+\epsilon_1\epsilon_2\int_{-\infty}^{\infty}dz\left(\frac{1}{\epsilon_{\parallel}}-\frac{1}{\epsilon_{\perp}}\right).\end{aligned} \tag{A 15}$$

At the Brewster angle θ_B, defined by $Q_1 = Q_2$ [9], $r_{p0} = 0$, $r_{s0} = (\epsilon_1 - \epsilon_2)/(\epsilon_1 + \epsilon_2)$ and the first order p-wave reflection amplitude becomes

$$r_{p1}(\theta_B) = -\frac{i}{2}\frac{\omega}{c}\frac{\epsilon_1\epsilon_2}{\sqrt{(\epsilon_1+\epsilon_2)}}D. \tag{A 16}$$

Equation (3) follows from (A 15) and (A 16).

Appendix B

Values of η_0 for some simple dielectric function profiles

We give analytic results for the integral

$$\eta_0 = \int_{-\infty}^{\infty} dz \frac{(\epsilon-\epsilon_1)(\epsilon-\epsilon_2)}{\epsilon} \tag{B 1}$$

for three simple functional forms of $\epsilon(z)$ (the first three of table 1, [26]). The dielectric function $\epsilon(z)$, with its limiting values $\epsilon(-\infty) = \epsilon_1$ and $\epsilon(\infty) = \epsilon_2$, is assumed to be real and positive everywhere. The form of (B 1) shows that η_0 is then negative definite if $\epsilon(z)$ is monotonic. The profiles are conveniently written in terms of a function f with limiting values ± 1 at $\pm\infty$:

$$\epsilon(z) = \tfrac{1}{2}(\epsilon_1+\epsilon_2) - \tfrac{1}{2}(\epsilon_1-\epsilon_2)f(z/a). \tag{B 2}$$

(Compare the expression (9) for the density.) The results are summarized in the following table :

Profile	$f(x)$	$-\eta_0/a$
Linear	$\begin{cases} x & (\lvert x\rvert<1) \\ \operatorname{sgn} x & (\lvert x\rvert>1) \end{cases}$	$\epsilon_1+\epsilon_2-\frac{2\epsilon_1\epsilon_2}{\epsilon_1-\epsilon_2}\log\frac{\epsilon_1}{\epsilon_2}$
Exponential	$\operatorname{sgn} x\,(1-\exp(-\lvert x\rvert))$	$\epsilon_1\log\frac{\epsilon_1+\epsilon_2}{2\epsilon_2}+\epsilon_2\log\frac{\epsilon_1+\epsilon_2}{2\epsilon_1}$
Hyperbolic tangent	$\tanh\frac{x}{2}$	$(\epsilon_1-\epsilon_2)\log\frac{\epsilon_1}{\epsilon_2}$

As $\epsilon_1 - \epsilon_2 \to 0$, the leading term in $-\eta_0$ is proportional to $(\epsilon_1-\epsilon_2)^2 a$, as is evident from the form of (B 1). The integrations leading to the values in the table are elementary, although the subtraction of two divergent integrals is useful in the case of the Fermi (or hyperbolic tangent) profile

$$\epsilon(z) = \frac{\epsilon_1}{1+\exp(z/a)} + \frac{\epsilon_2}{1+\exp(-z/a)} = \frac{\epsilon_1+\epsilon_2\exp(z/a)}{1+\exp(z/a)}, \tag{B 3}$$

for which we have :

$$-\eta_0/a = (\epsilon_1-\epsilon_2)^2 \int_{-\infty}^{\infty} dr \frac{\exp x}{1+\exp x}\frac{1}{\epsilon_1+\epsilon_2\exp x}$$

$$= (\epsilon_1-\epsilon_2)^2 \int_0^{\infty} dy \frac{1}{1+y}\frac{1}{\epsilon_1+\epsilon_2 y}$$

$$= (\epsilon_1 - \epsilon_2) \lim_{Y \to \infty} \int_0^Y dy \left\{ \frac{1}{1+y} - \frac{1}{\frac{\epsilon_1}{\epsilon_2} + y} \right\}$$

$$= (\epsilon_1 - \epsilon_2) \log \frac{\epsilon_1}{\epsilon_2}. \tag{B 4}$$

The Fermi profile has the useful property that when the density has a Fermi shape, the Clausius–Mossotti functional form for $\epsilon(z)$ also has a Fermi shape, shifted toward the denser medium : when

$$n(z) = \frac{n_1 + n_v \exp(z/a)}{1 + \exp(z/a)}, \tag{B 5}$$

$$\epsilon_{CM}(z) = \frac{\epsilon_1 + \epsilon_v \exp[(z+\Delta)/a]}{1 + \exp(z+\Delta)/a]}, \tag{B 6}$$

where

$$\Delta = a \log \left(\frac{1 - \frac{4}{3}\pi\alpha n_v}{1 - \frac{4}{3}\pi\alpha n_1} \right) = a \log \left(\frac{\epsilon_1 + 2}{\epsilon_v + 2} \right). \tag{B 7}$$

Since η is invariant to change of origin, (B 4) applies to the profile (B 6). Other profiles have a similar (though approximate) shift of the Clausius–Mossotti functional form relative to the density : figure 1 of [2] illustrates the shift for an exponential density profile.

References

[1] Lekner, J., and Castle, P. J., 1980, *Physica* A, **101,** 89.
[2] Castle, P. J., and Lekner, J., 1980, *Physica* A, **101,** 99.
[3] Jasperson, S. N., and Schnatterly, S. E., 1969, *Rev. scient. Instrum.*, **40,** 761.
[4] Beaglehole, D., 1980, *Physica* B, **100,** 163.
[5] Drude, P., 1959, *The Theory of Optics* (Dover), pp. 287–295.
[6] Lorenz, L., 1860, *Annln Phys.*, **111,** 460.
[7] Rayleigh, J. W. S., 1912, *Proc. R. Soc.*, **86,** 207.
[8] Zielinska, B. J. A., Bedeaux, D., and Vlieger, J., 1981, *Physica* A, **107,** 91. Zielinska, B. J. A., and Bedeaux, D., 1982, *Physica* A, **112,** 265.
[9] Lekner, J., 1982, *Physica* A, **113,** 506.
[10] Buff, F. P., 1966, *Saline Water Conversion Report* (U.S. Govt. Printing Office, Washington D.C.), p. 26.
[11] Abelès, F., 1976, *Thin Solid Films*, **34,** 291.
[12] Amey, R. L., and Cole, R. H., 1964, *J. chem. Phys.*, **40,** 146. Abbiss, C. P., Knobler, C. M., Teague, R. K., and Pings, C. J., 1965, *J. chem. Phys.*, **42,** 4145. Garside, D. H., Molgaard, H. V., and Smith, B. L., 1968, *J. Phys.* B, **1,** 449. Chan, M., Ryschkewitsch, M., and Meyer, H., 1977, *J. low-temp. Phys.*, **26,** 211.
[13] Lekner, J., and Henderson, J. R., 1980, *Molec. Phys.*, **39,** 1437.
[14] Verlet, L., 1968, *Phys. Rev.*, **165,** 201.
[15] McDonald, I. R., and Singer, K., 1972, *Molec. Phys.*, **23,** 29. Freeman, K. S. C., and McDonald, I. R., 1973, *Molec. Phys.*, **26,** 529.
[16] National Standard Reference Data Monograph 27, 1969, National Bureau of Standards, Washington, D.C.
[17] Cook, G. A. (editor), 1961, *Argon, Helium and the Rare Gases*, Vol. I (Interscience), p. 360.
[18] Streett, W. B., Sagan, L. S., and Staveley, L. A. K., 1973, *J. Chem. Thermo.*, **5,** 633.

[19] PORTIS, A. M., 1978, *Electromagnetic Fields : Sources and Media* (John Wiley), p. 80.
[20] SHIH, C. C., and UANG, Y. H., 1978, *Phys. Rev.* A, **17,** 377.
[21] HENDERSON, J. R., and LEKNER, J., 1979, *Phys. Rev.* A, **20,** 621.
[22] LEKNER, J., and HENDERSON, J. R., 1977, *Molec. Phys.*, **34,** 333.
[23] LEKNER, J., and HENDERSON, J. R., 1978, *Physica* A, **94,** 545.
[24] WIDOM, B., 1972, *Phase Transitions and Critical Phenomena*, Vol. 2, edited by C. Domb and M. S. Green (Academic Press), p. 79.
[25] THOMPSON, S. M., and GUBBINS, K. E., 1981, *J. chem. Phys.*, **74,** 6467. THOMPSON, S. M., GUBBINS, K. E., and HAILE, J. M., 1981, *J. chem. Phys.*, **75,** 1325. SLUCKIN, T. J., 1982, *Molec. Phys.*, **47,** 267.
[26] LEKNER, J., 1982, *Physica* A, **112,** 544.
[27] LANDAU, L. D., and LIFSHITZ, E. M., 1960, *Electrodynamics of Continuous Media* (Pergamon), § 68.